Journal: Nature Medicine SI Guide

Article Title:	Dynamic regulation of cardiolipin by the lipid pump, ATP8b1, determines the severity of lung injury in experimental bacterial pneumonia Nancy B. Ray, Lakshmi Durairaj, Bill B. Chen, Bryan J. McVerry, Alan J. Ryan, Michael Donahoe, Alisa K. Waltenbaugh, Christopher P. O'Donnell, Florita C. Henderson, Christopher A. Etscheidt, Diann M. McCoy, Marianna Agassandian, Emily C. Hayes-Rowan, Tiffany A. Coon, Phillip L. Butler,Lokesh Gakhar, Satya N. Mathur, Jessica C. Sieren, Yulia Y. Tyurina, Valerian E. Kagan, Geoffrey McLennan, and Rama K. Mallampalli
Corresponding Author:	**Rama K. Mallampall**i

Supplementary Item & Number	**Title or Caption**
Supplementary Table 1	Subject clinical characteristics
Supplementary Figure 1	Bacterial pathogen and duration of mechanical ventilation do not affect tracheal aspirate cardiolipin (CL) levels
Supplementary Figure 2	BAL protein, cytokines and cell counts and lung surfactant proteins in cardiolipin (CL) treated mice
Supplementary Figure 3	ATP8b1 expression
Supplementary Figure 4	ATP8b1 overexpressing mice
Supplementary Figure 5	BAL proteins and cell counts, lung edema and bacterial load in ATP8b1 defective mice
Supplementary Figure 6	BAL cytokines, lung surfactant proteins and lung mechanics in ATP8b1 defective mice
Supplementary Figure 7	Mapping the cardiolipin (CL) binding motif within ATP8b1
Supplementary Figure 8	BAL cell counts, proteins and cytokines in mice given cardiolipin binding domain (CBD) peptide
Supplementary Figure 9	Surfactant proteins, apoptosis and lung mechanics in mice given cardiolipin binding domain (CBD) peptide
Supplementary Figure 10	Assessment of cardiolipin (CL) molecular species in patients with pneumonia and mice challenged with *E. coli*
Supplementary Figure 11	ATP8b1 degradation and ubiquitination
Supplementary Figure 12	Cardiolipin (CL) uptake is not regulated by related P-type ATP pumps
Supplementary Figure 13	Cardiolipin (CL) and CL binding domain peptide regulate cell survival pathways
Supplementary Methods	Methods

Table 1 – Subject clinical characteristics

	Nonpulmonary Critical Illness (n=5)	Pneumonia (n=17)	Congestive Heart Failure (n=6)
Age (Mean, SD)	44 ± 15	47 ± 20	59 ± 19
Female (%)[a]	100	29	67
Days on Mechanical Ventilation [Median,(IQR)][b]	2 (2,4)	4 (3,13)	3 (2,6)
Antibiotic Use (%)	100	100	67
Aspirate Culture (% positive)[b]	0	64.7	16.7[c]
No Growth	40	35.3	33.3
Staphylococcus aureus		17.6	16.7
Streptococcus pneumoniae		23.5	
Pseudomonas aeruginosa		17.6	
Haemophilus influenzae		5.9	
Candida albicans	60		
Culture not sent			50

[a] $P<0.05$ by Kruskal-Wallis test

[b] Data presented in Supplementary Figure 1

[c] Subjects in whom cultures not sent included as culture negative

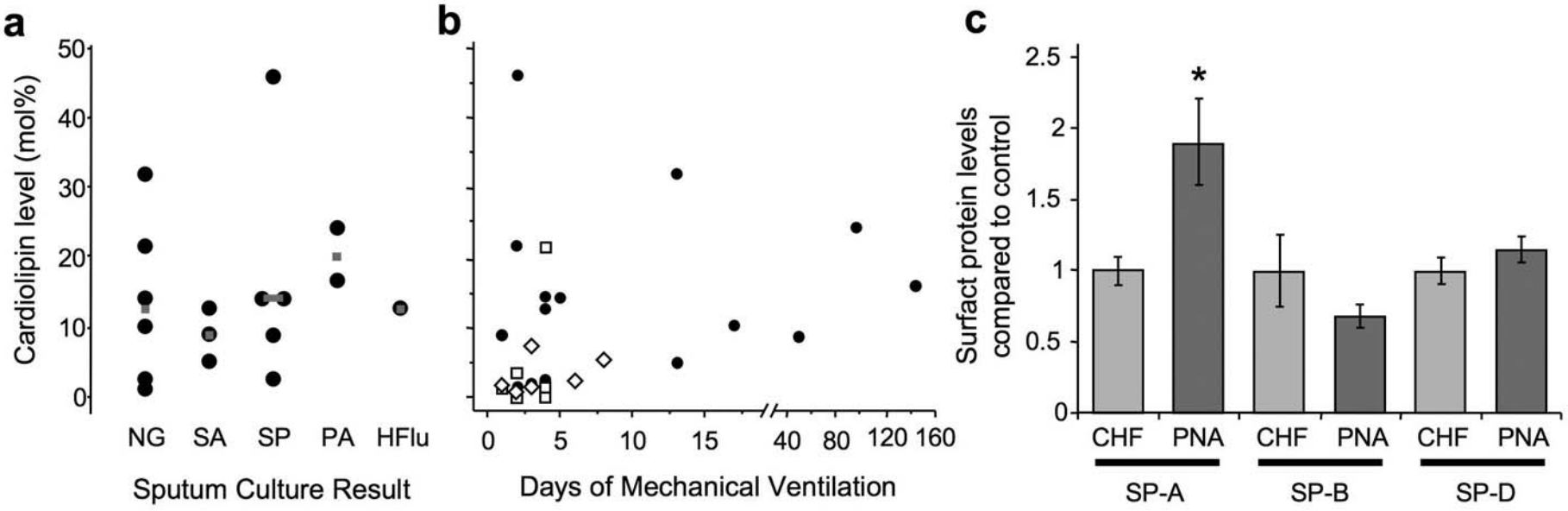

Figure 1. **Bacterial pathogen and duration of mechanical ventilation do not affect tracheal aspirate cardiolipin (CL) levels.** Panel **a** depicts tracheal aspirate CL levels (median (gray dashes)) from patients with pneumonia (n=17) categorized according to tracheal aspirate culture results (NG - no growth, SA – *Staphylococcus aureus*, SP – *Streptococcus pneumonia*, PA – *Pseudomonas aeruginosa*, HFlu – *Haemophilus influenzae*). Panel **b** depicts tracheal aspirate CL levels from all patients enrolled in the study (nonpulmonary critical illness [NPCI] open squares n=6, pneumonia [PNA] black circles n=17, congestive heart failure [CHF] open diamonds n=6) categorized by days on mechanical ventilation when the sample was collected. Panel **c** depicts tracheal aspirate surfactant associated protein quantification (mean ± SEM) in pneumonia (PNA, n=17) compared to CHF (n=6) patients. *P<0.05 by ANOVA.

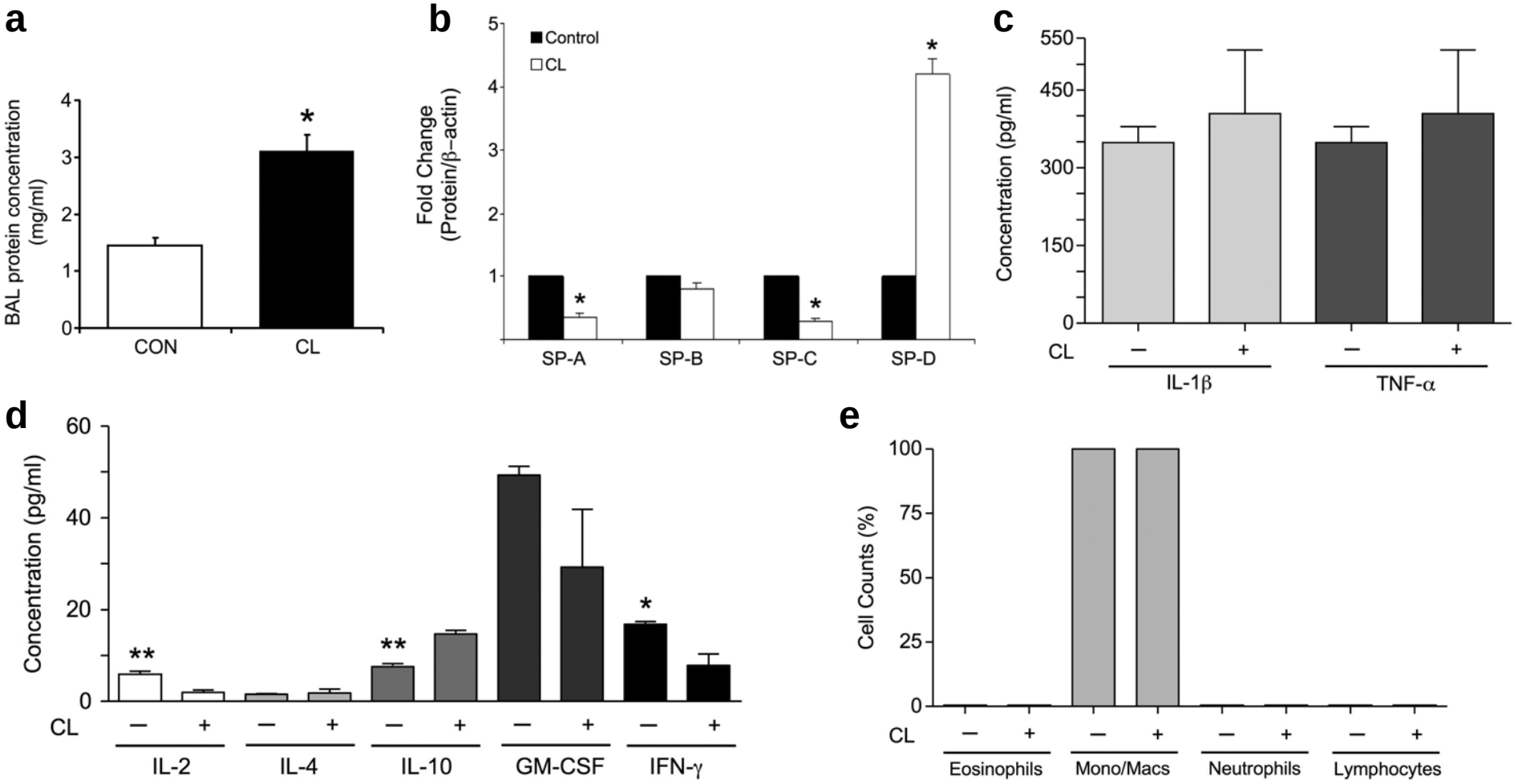

Figure 2. **BAL protein, cytokines and cell counts and lung surfactant proteins in cardiolipin (CL) treated mice.**
a) Mice (n=5 group) were given diluent (CON) or CL (50 nmol, i.t.) for 1 h. BAL supernatants were assayed for protein concentration using a Lowry assay. **P*<0.05 vs. control. **b**) Mice given i.t. CL (50 nmol) were euthanized, lungs removed and used for immunoblotting using SP-A, SP-B, SP-D antibodies from Millipore and SP-C from ABCAM. Densitometry of three to five separate experiments was performed and expressed as fold change from control (β-actin). **P*<0.05 vs. control. **c, d**) Mice (n=3 group) were given CL (50 nmol, i.t.) for 1 h. BAL was collected and centrifuged. 0.5% fatty-acid free BSA plus EDTA-free protease inhibitor cocktail was added to the supernatant. 50 ul of supernatant was assayed for cytokines with a Bio-Plex Mouse Assay 8-Plex Group 1 kit (BioRad). ***P*<0.01 for IL-2 control vs. IL-2 CL, and IL-10 control vs. IL-10 CL, **P*<0.05 for IFN-γ control vs. IFN- γ CL. **e**) Mice (n=5 group) were given CL (50 nmol, i.t.) for 1 h. BAL were collected and centrifuged. Cells from pellets were resuspended in Hanks BSS and 1 x 10^5 cells were Cyto-spun onto slides and stained with Wright-Giemsa stain for differential cell counting.

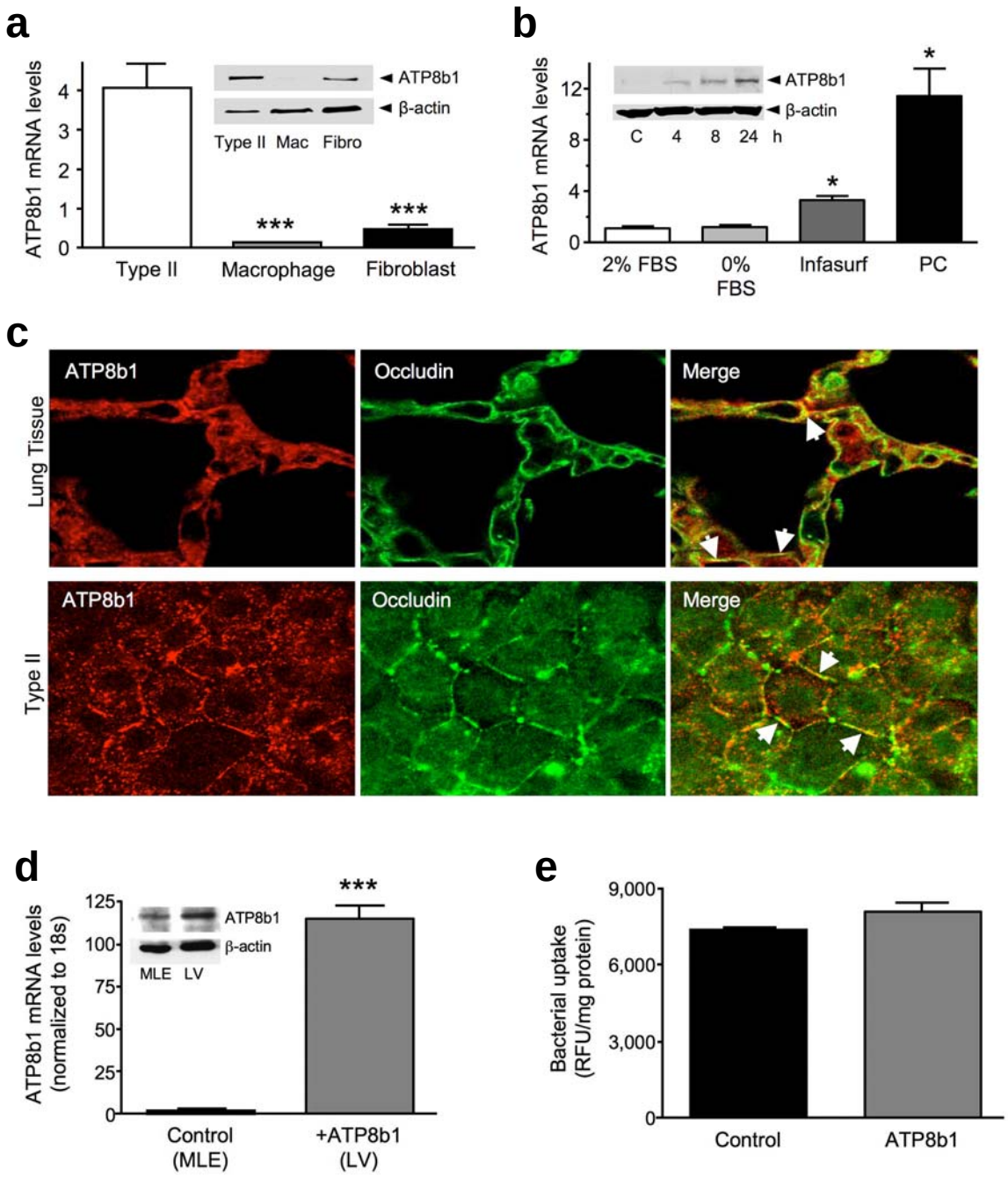

Figure 3**. ATP8b1 expression**.
a) ATP8b1 is highly expressed in alveolar epithelium. Real-time PCR reveals significantly higher ATP8b1 mRNA expression and immunoreactive protein (inset) in primary type II epithelial cells versus alveolar macrophages or fibroblasts. RNA levels were normalized to 18S. **b**) MLE cells were cultured with 120 nmol of Infasurf or PC liposomes for at least 4 h and processed for ATP8b1 mRNA expression and protein (inset). In **a-b**, significance was determined by a one-way ANOVA where **P*<0.05 and ****P*<0.001. **c**) Frozen lung sections from murine lung tissue (top row) and primary type II cells (lower row) isolated from (n=3 animals) were processed for immunostaining using rabbit anti-ATP8b1 or mouse anti-occludin primary antibodies followed by AlexaFlour 568 goat anti-rabbit and AlexaFluor488 chicken anti-mouse secondary antibodies, respectively. **d**) ATP8b1 overexpressing cells. A lentiviral transduced V5-ATP8b1 stable cell line was analyzed for ATP8b1 mRNA by quantitative PCR and V5-immunoreactive protein (inset). **e**) MLE cells were infected with empty adenovirus or Ad5-ATP8b1. Cells were then exposed to GFP-labeled *E. coli* (5×10^7 CFU) for 1 h. Cells were harvested and lysates were collected. GFP levels in the lysates were quantified and normalized to the total amount of protein.

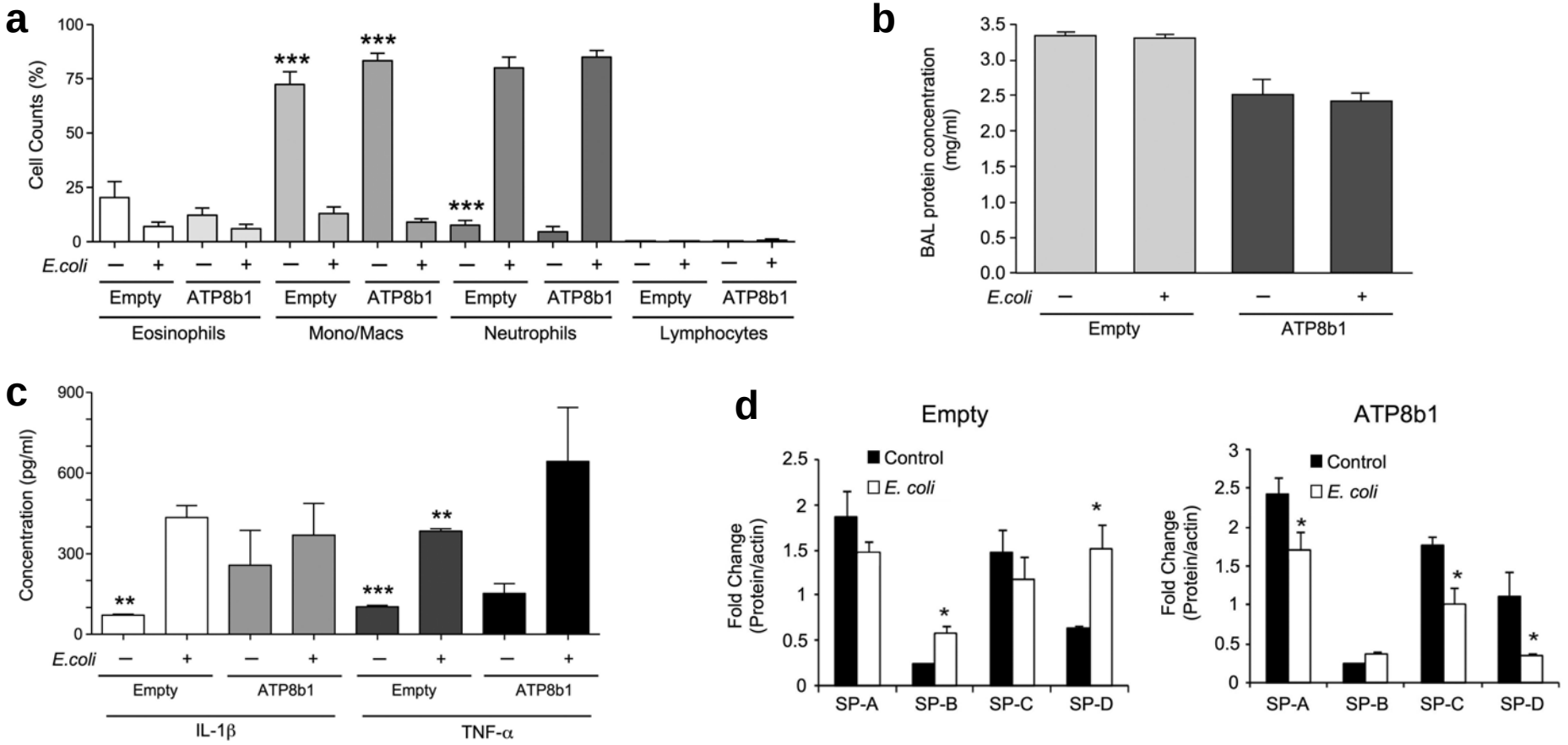

Figure 4. **ATP8b1 overexpressing mice.**
Mice were infected with Ad5 (empty) or Ad5-ATP8b1 (n=3-4 group) and then inoculated with 1 x 10^6 CFU *E. coli* or uninfected for 48 h. BAL were collected and centrifuged. **a**) Cell counts in ATP8b1 overexpressing mice. Cells from pellets were resuspended in Hanks BSS and 1 x 10^5 cells were Cyto-spun onto slides and stained with Wright-Giemsa stain for differential cell counting. Mono/Macs and Neutrophils: ***P<0.001 for comparisons between empty vs. empty + *E. coli*, empty vs. ATP8b1 + *E. coli*, ATP8b1 vs. ATP8b1 + *E. coli*. **b**) BAL protein in ATP8b1 overexpressing mice. BAL supernatants were assayed for protein concentration using a Lowry assay. **c**) 0.5% fatty-acid free BSA plus EDTA-free protease inhibitor cocktail was added to the supernatant and assayed for cytokines with a Bio-Plex Mouse Assay 8-Plex Group 1 kit (BioRad). **P<0.01 for IL-1β empty vs. IL-1β + *E. coli*, TNFα empty + *E. coli* vs. TNFα ATP8b1, ***P<0.001 for TNFα empty vs. TNFα empty + *E. coli*. **d**) Surfactant proteins in the lungs were assayed by immunoblotting using SP-A, SP-B, SP-D antibodies from Millipore and SP-C from ABCAM. Densitometry of three to five separate experiments was performed and expressed as fold change from control (β-actin). *P<0.05 vs. control. **e**) Lung mechanics in ATP8b1 overexpressing mice. Mice (n=8/group) received an empty vector (Ad5) or Ad5-ATP8b1 (2.5 x 10^8 PFU) i.t. and 24 h later given *E. coli* at 10^6 CFU/mouse for 48 h. Animals were anesthetized, paralyzed and mechanically ventilated and lung resistance determined as in Fig. 2. Significance was determined by a one-way ANOVA where *P<0.05 for Ad5 + *E. coli* vs. Ad5-ATP8b1, **P<0.01 for Ad5 + *E. coli* vs. Ad5-ATP8b1+ *E. coli*.

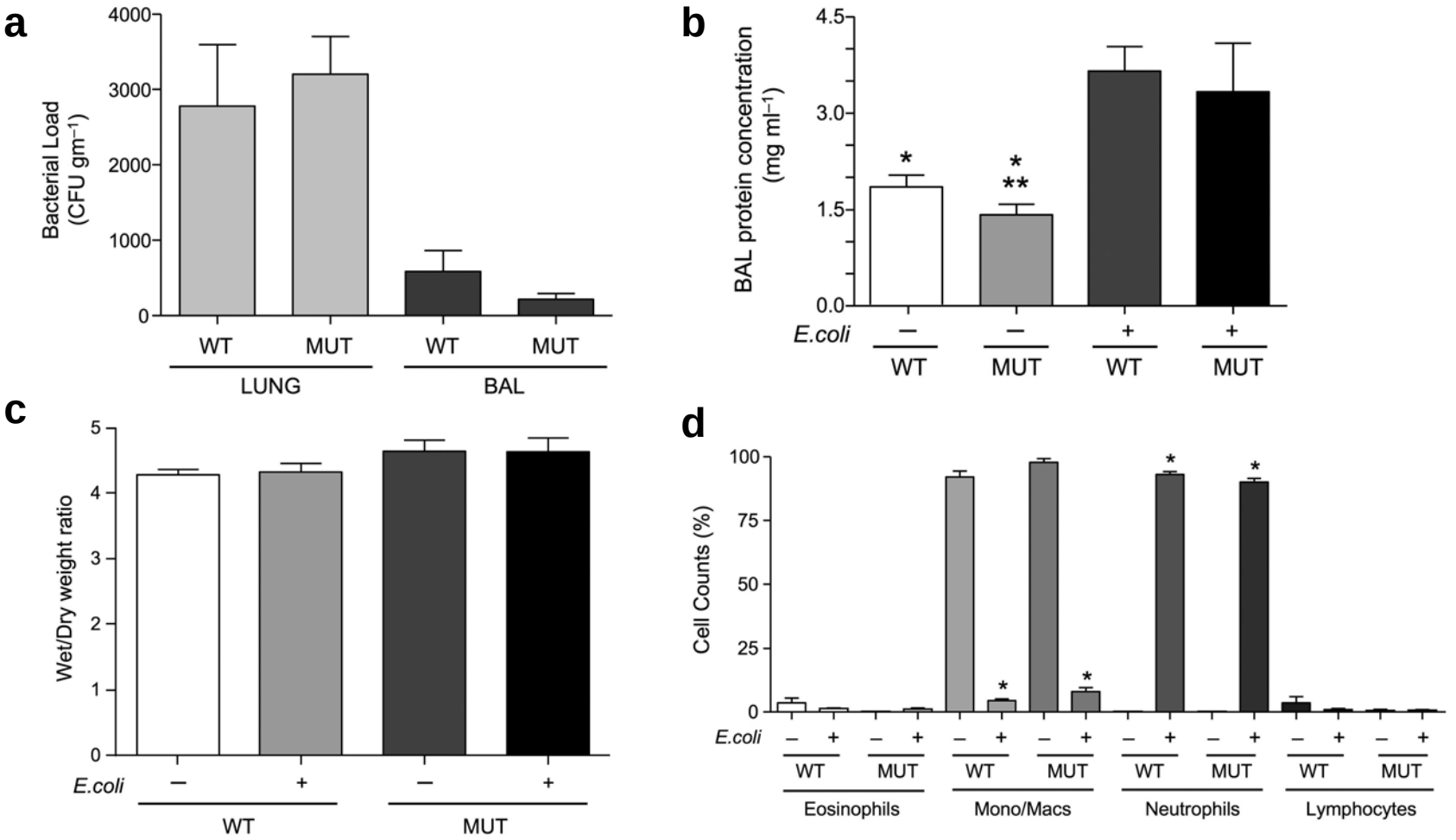

Figure 5. **BAL proteins and cell counts, lung edema and bacterial load in ATP8b1 defective mice.**
a) Bacterial loads in ATP8b1 defective mice. ATP8b1 mutant (MUT) mice and wild-type (WT) littermates (n=4 group) (129S strain) were inoculated with 1 x 10^6 CFU *E. coli*. Lungs were lavaged with PBS after 48 h, lungs resected and homogenized. BAL supernatants and lung homogenates were diluted and plated on TSB agar plates to determine colony forming units (CFU). **b**) BAL protein in ATP8b1 defective mice**.** BAL supernatants from MUT and WT mice (6 per group), were assayed for protein concentration using a Lowry assay. **P*<0.05 for WT vs WT + *E. coli*, and MUT vs. MUT+ *E. coli*, ***P*<0.01 for MUT vs WT+ *E. coli*. **c**) Lung edema in ATP8b1 defective mice**.** ATP8b1 mutant (MUT) mice and wild-type (WT) littermates (n=4 mice/group) were inoculated with 1 x 10^6 CFU *E. coli* or uninfected for 48 h. Lungs were removed after 48 hr, blotted, and placed in tared weigh boats and weighed. The lungs were then dried for 24 h at 60 °C in the same weigh boats and weighed again. **d**) Cell counts in ATP8b1 defective mice. BAL from MUT and WT (n=6 per group) were collected and centrifuged. Cells from pellets were resuspended in Hanks BSS and 1 x 10^5 cells were Cyto-spun onto slides and stained with Wright-Giemsa stain for differential cell counting. **P*<0.05 vs. uninfected groups.

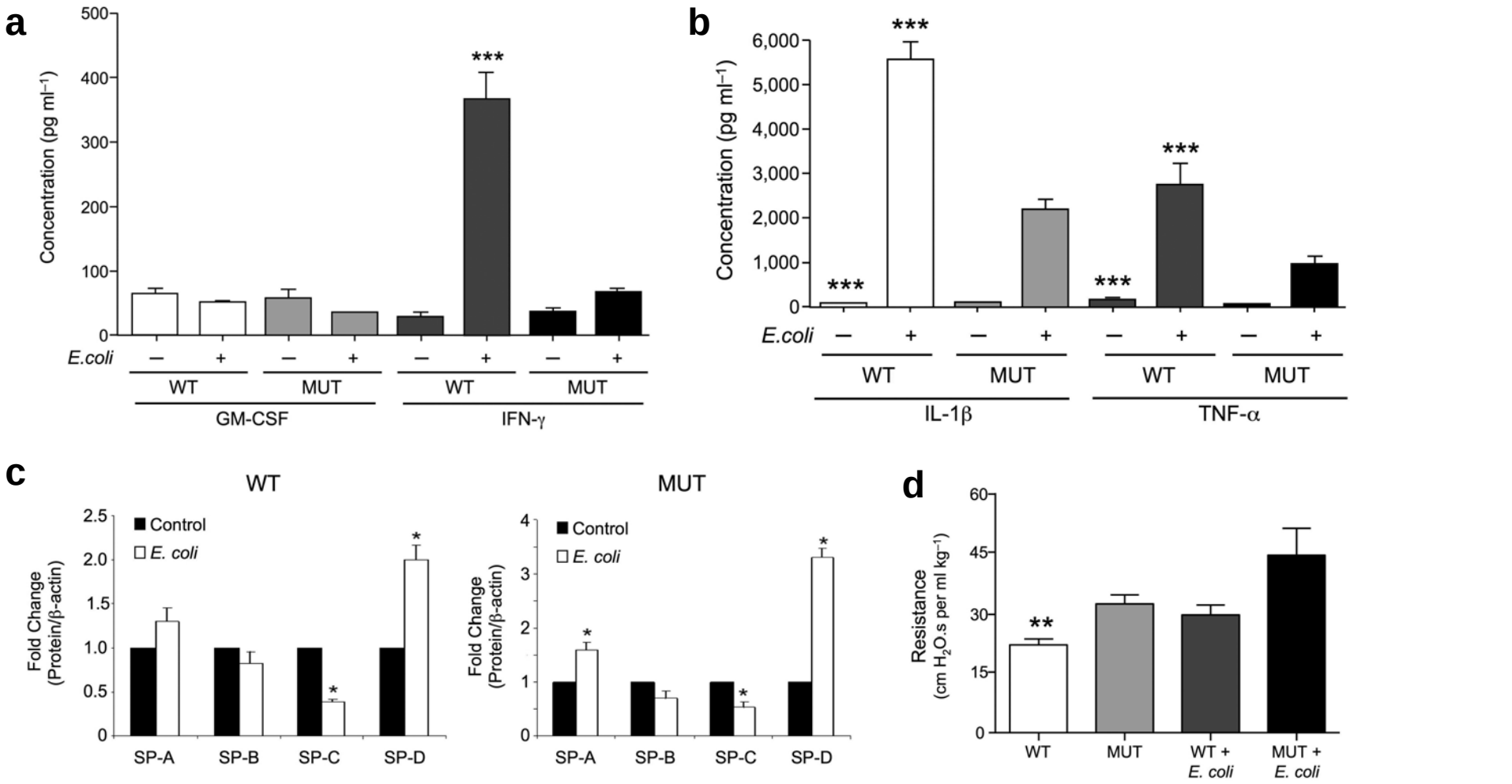

Figure 6. **BAL cytokines, lung surfactant proteins and lung mechanics in ATP8b1 defective mice.**
a, b) **Cytokines** in ATP8b1 defective mice. ATP8b1 mutant (MUT) mice and wild-type (WT) littermates (n=4 group) were infected with 1 x 10^6 CFU *E. coli* or uninfected for 48 h. BAL was collected and centrifuged. 0.5% fatty-acid free BSA plus EDTA-free protease inhibitor cocktail was added to the supernatant which was assayed for cytokines with a Bio-Plex Mouse Assay 8-Plex Group 1 kit (BioRad). a) ***P<0.001 for IFN-γ WT uninf vs. IFN-γ WT inf, IFN-γ WT inf vs. IFN-γ MUT uninf, and IFN-γ WT inf vs. IFN-γ MUT inf. b) ***P<0.001 for IL-1β WT uninf vs. IL-1β WT inf, IL-1β WT uninf vs. IL-1β MUT inf, IL-1β WT inf vs. IL-1β MUT uninf, IL-1β WT inf vs. IL-1β MUT inf, TNF-α WT uninf vs. TNF-α WT inf, TNF-α WT inf vs. TNF-α MUT uninf, and TNF-α WT inf vs. TNF-α MUT inf. **c**) **Surfactant proteins** in the lungs of wild type and ATP8b1 mutant mice with and without *E.coli* infection were assayed by immunoblotting using SP-A, SP-B, SP-D antibodies from Millipore and SP-C from ABCAM. Densitometry of three to five separate experiments was performed and expressed as fold change from control (β-actin). *P<0.05 vs. control. **d**) ATP8b1G308V/G308V mutants and wild-type littermates uninfected (n=7/group) or infected (n=7/group) with *E. coli* at 10^6 CFU/mouse for 48 h were analyzed for resistance. Mice were mechanically ventilated for determination of resistance. Statistical significance was determined by a one-way ANOVA where **P<0.01 for WT vs. MUT + *E.coli*, and WT vs. MUT.

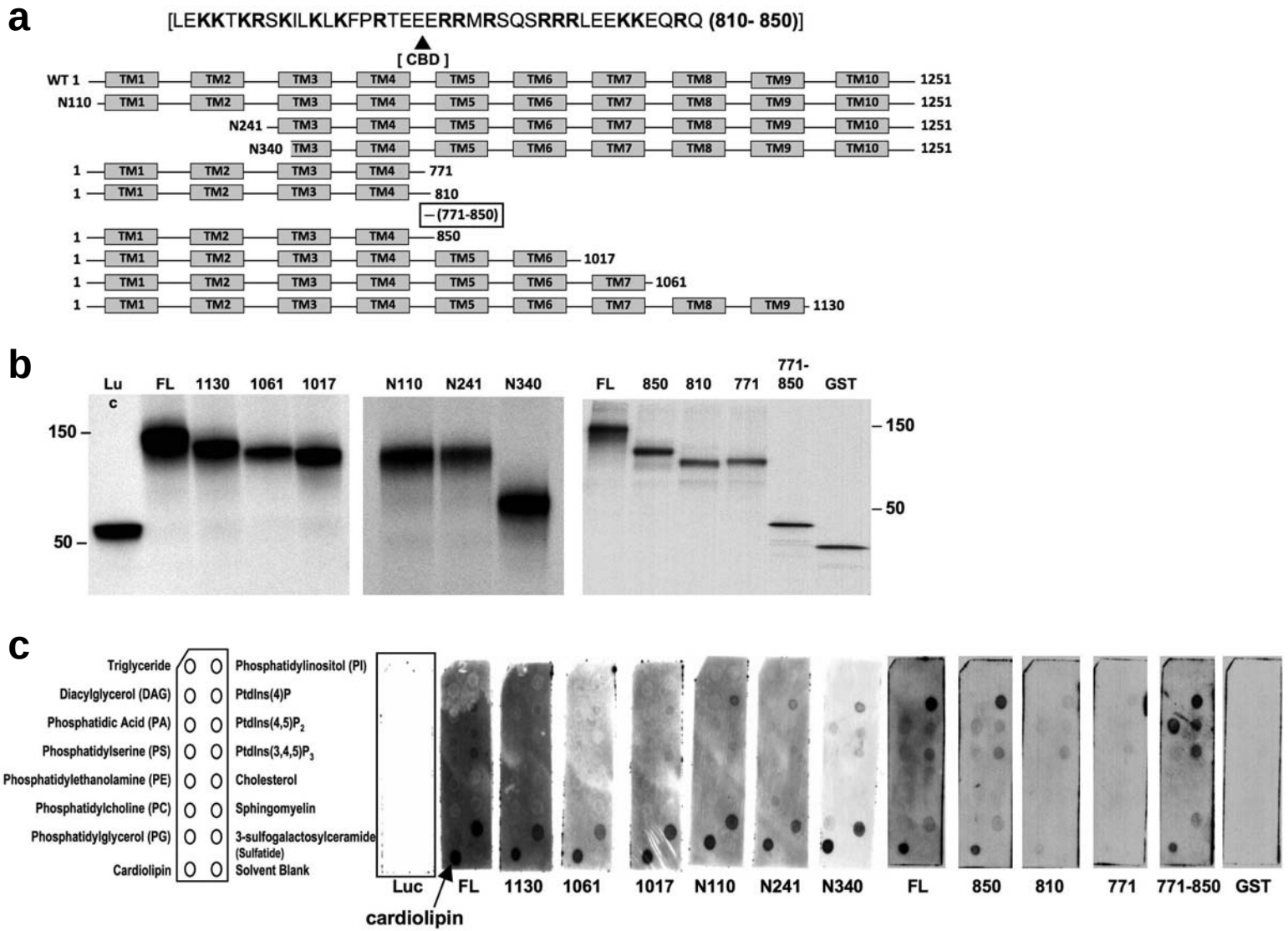

Figure 7. **Mapping the cardiolipin (CL) binding motif within ATP8b1.**

a) Map of full-length (FL) (1251 amino acids) ATP8b1, NH_2-terminal deletion mutants (amino acid start sequence number preceded by N), a mutant encoding residues 771-850, and carboxyl-terminal truncation mutants (amino acid number truncation site). **b**) FL, mutant, and luciferase control protein was expressed using *in vitro* translation using ^{35}S-methionine and reaction products resolved by SDS PAGE. **c**) Labeled proteins were incubated with lipid strips pre-spotted with fifteen lipids (far left map) including CL (shown with arrow)**.** Luciferase (Luc) and GST served as negative controls. Each ATP8b1 mutant was tested for lipid association in at least n=3 separate experiments. The CL binding domain (CBD) is a basic amino acid enriched (bold lettering) motif shown at the top of **a** and spans residues 810-850.

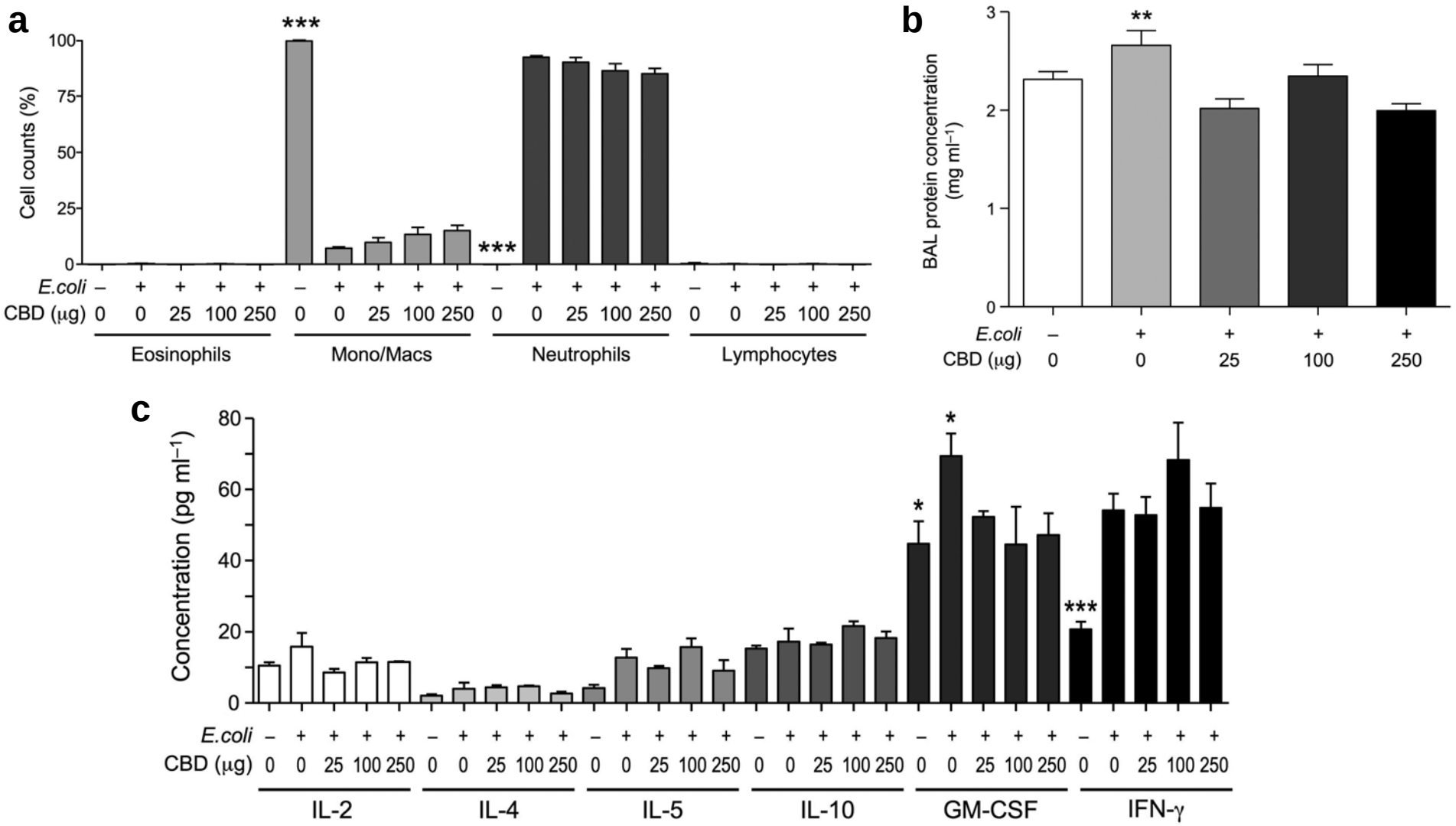

Figure 8. **BAL cell counts, proteins and cytokines in mice given cardiolipin binding domain (CBD) peptide.**
a) Cell counts in mice given CBD peptide. Mice were inoculated with 1 x 10^6 CFU *E. coli* or uninfected for 48 h prior to i.t. administration of various amounts of CBD. BAL were collected and centrifuged. Cells from pellets were resuspended in Hanks BSS and 1 x 10^5 cells were Cyto-spun onto slides and stained with Wright-Giemsa stain for differential cell counting. Mono/Macs and Neutrophils: ****P*<0.001 for control (0-) vs. vehicle buffer (0+), 25 μg CBD, 100 μg CBD, or 250 μg CBD. **b**) **BAL protein in mice given CBD peptide.** Mice (n=5-6 mice/ group) were infected with *E. coli* at 10^6 CFU/mouse. After 48 h, mice were given CBD (50 nmol, i.t.) for 1 h. BAL supernatants were assayed for protein concentration using a Lowry assay. ***P*<0.01 for vehicle buffer (0+) vs. 25 μg CBD and 250 μg CBD. **c**) **Cytokines in mice given CBD peptide.** Mice (n=4/group) were inoculated with 1 x 10^6 CFU *E. coli* or uninfected for 48 h prior to i.t. administration of CBD. Mice were lavaged, BAL were collected and centrifuged. Supernatant were assayed for cytokines with a Bio-Plex Mouse Assay 8-Plex Group 1 kit (BioRad). **P*<0.05 for control (0-) vs. vehicle buffer (VB, 0+) + *E. coli*, VB + *E. coli* vs. 25 μg CBD + *E. coli,* VB + *E. coli* vs. 100 μg CBD + *E. coli*, VB + *E. coli* vs. 250 μg CBD + *E. coli*, ****P*<0.001 for control vs. VB, 25 μg, 100 μg, and 250 μg CBD + *E. coli*.

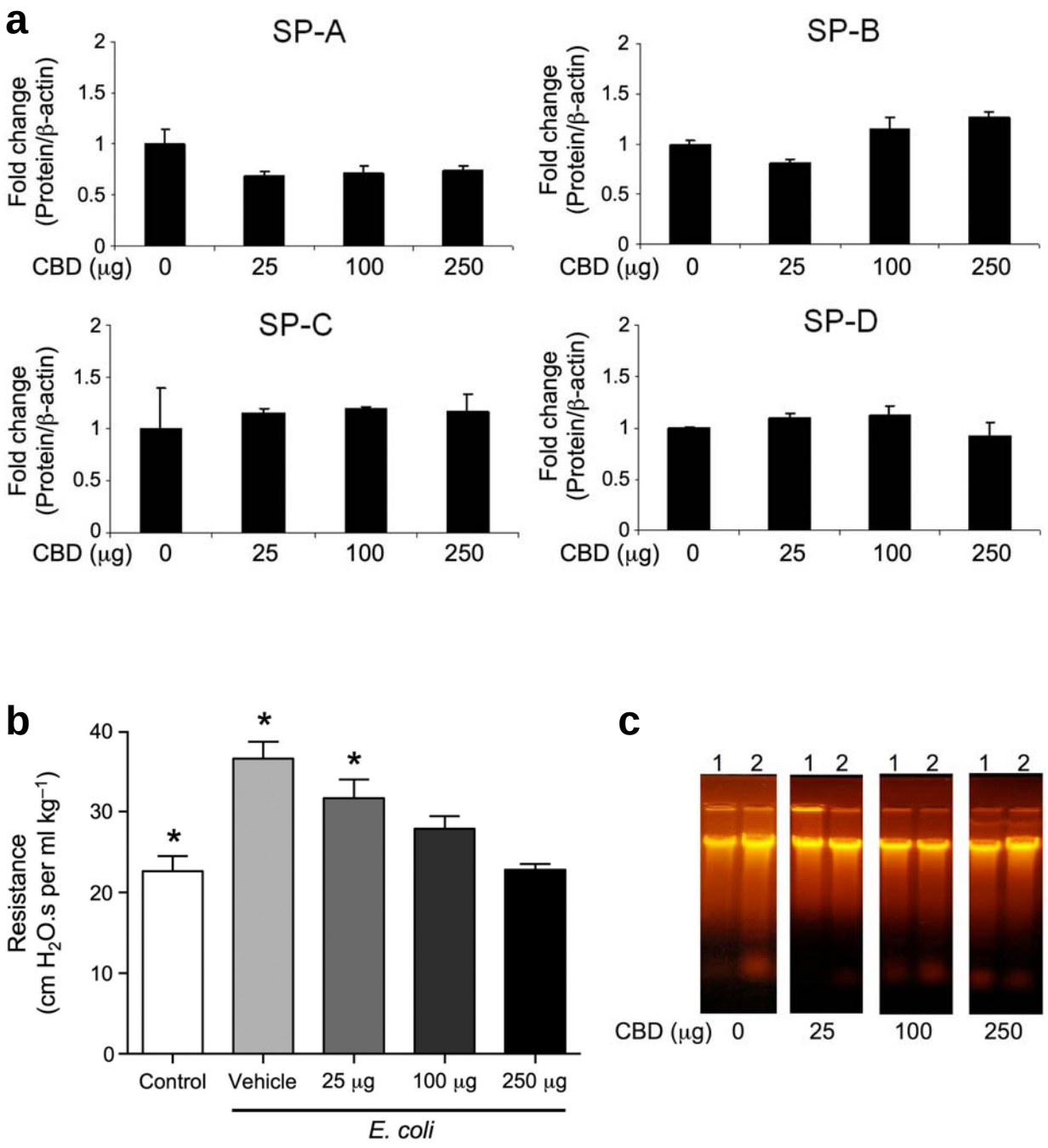

Figure 9**. Surfactant proteins, apoptosis and lung mechanics in mice given cardiolipin binding domain (CBD) peptide.**
a) **Surfactant proteins**. Mice were given i.t. CBD peptide after *E. coli* infection. Lungs were assayed by immunoblotting using SP-A, SP-B, SP-D antibodies from Millipore and SP-C from ABCAM. Densitometry of three to five separate experiments was performed and expressed as fold change from control (β-actin). **b**) **Lung mechanics in mice given CL binding domain peptide**. C57/BL6 mice (n=6 mice/group) were uninfected (control) or given *E. coli* at 10^6 CFU/mouse. After 48 h, mice were given vehicle, or 25 μg–250 μg of CBD peptide into lungs using a microsprayer aerosolizer. After 10 min, biophysical measurements were taken in mechanically ventilated mice for determination of resistance. Significance was determined by a one-way ANOVA. **P*<0.05 for control vs. vehicle and 25 μg; vehicle vs. 100 μg and 250 μg; and 25 μg vs. 250 μg. **c**) Mice treated as in (**b**) were also analyzed for lung DNA fragmentation.

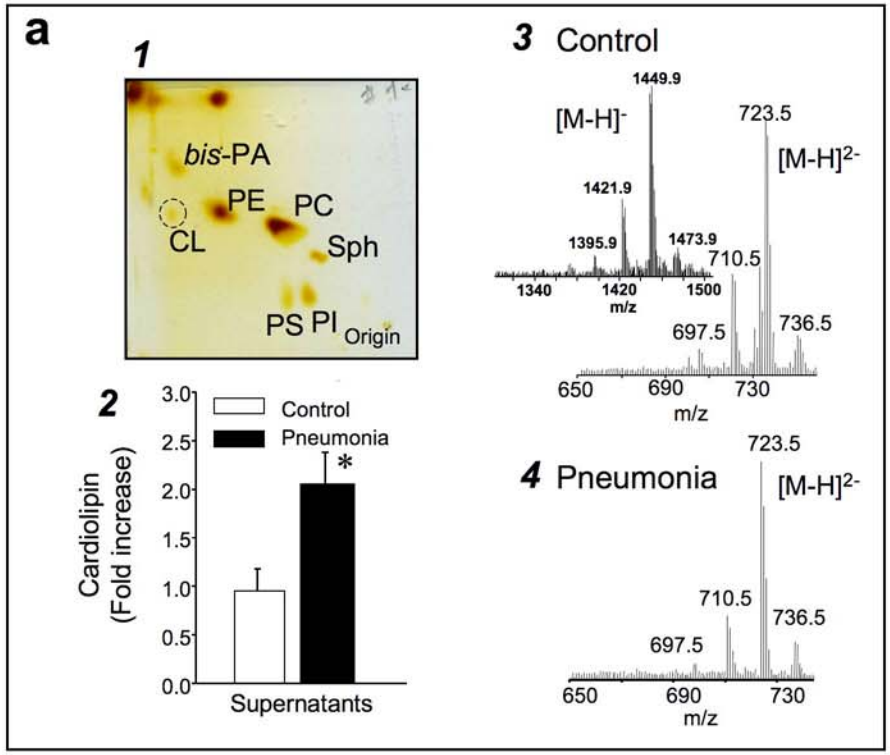

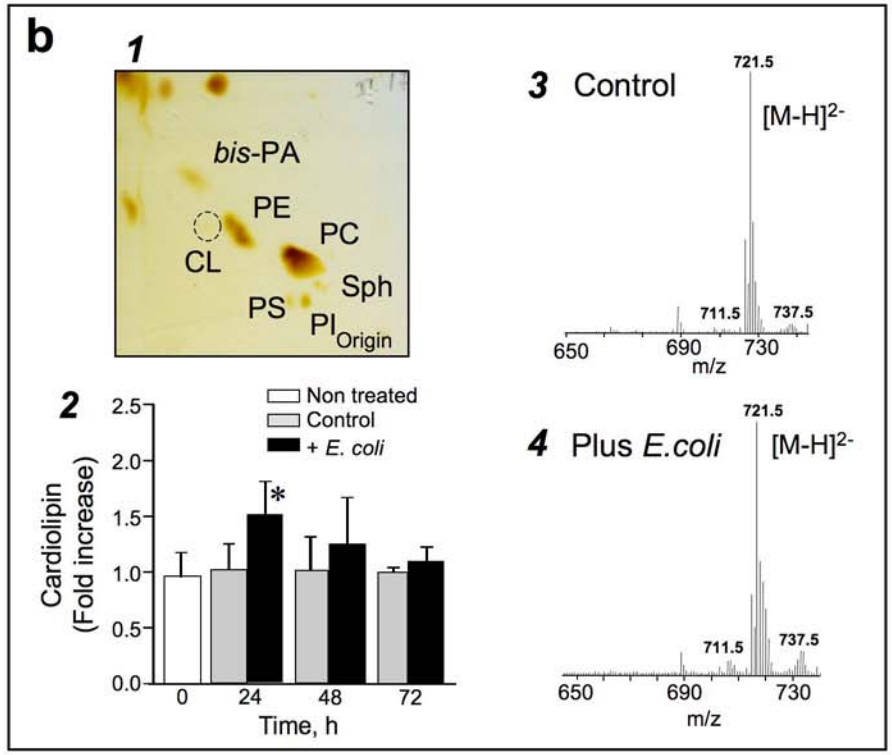

c

CL molecular species from human and mouse BAL

$[M-H]^{2-}$ m/z	$[M-H]^{-}$ m/z	C:DB	Molecular species	
698.5	1395.9	68:6	C16:1/C16:1/C18:2/C18:2	Human BAL
710.5	1421.9	70:7	C16:1/C18:2/C18:2/C18:2	Human/mouse BAL
711.5	1423.9	70:6	C16:1/C18:1/C18:2/C18:2	Human/mouse BAL
719.5	1443.9	72:10	C18:3/C18:2/C18:2/C18:3	Mouse BAL
721.5	1445.9	72:9	C18:3/C18:2/C18:2/C18:2	Mouse BAL
723.5	1447.9	72:8	C18:2/C18:2/C18:2/C18:2	Human BAL
724.5	1449.9	72:7	C18:1/C18:2/C18:2/C18:2	Human BAL
725.5	1452.9	72:6	C18:1/C18:1/C18:2/C18:2	Human BAL
736.5	1473.9	74:9	C18:1/C18:2/C18:2/C20:4	Human/mouse BAL
737.5	1475.9	74:8	C18:1/C18:1/C18:2/C20:4	Human/mouse BAL

C:DB – carbon:double bond ratio

Figure 10. **Assessment of cardiolipin (CL) molecular species in patients with pneumonia and mice challenged with *E.coli.***
a) Detection and quantitative assessment of cardiolipin in supernatants obtained from bronchoalveolar lavage (BAL) of healthy subjects and patients with pneumonia. (*a.1*) Typical 2D-HPTLC of total lipids extracted from BAL of healthy subject. PC, phosphatidylcholine, PE, phosphatidylethanolamine, PS, phosphatidylserine, PI, phosphatidylinositol, CL, cardiolipin, Sph, sphingomyelin, bis-PA, bis-phosphatidic acid. (*a.2*) Cardiolipin content in supernatants obtained from BAL of healthy subjects and patients with pneumonia. Data are mean ± SEM. **P*<0.03 vs. control, n=3 for control, n=5 for pneumonia. (*a.3-a.4*) Typical negative ESI-MS spectra of doubly-charged ($[M-H]^{2-}$) cardiolipin obtained from a healthy subject (*a.3*) and a patient with pneumonia (*a.4*). In addition typical spectrum of singly charged ($[M-H]^{-}$) cardiolipin from a healthy subject is shown (*a.3, insert*). **b**) Detection and quantitative assessment of cardiolipin in BAL of control mice and mice treated with *E.coli*. (*b.1*) Typical 2D-HPTLC of total lipids extracted from BAL of control mice. PC, phosphatidylcholine, PE, phosphatidylethanolamine, PS, phosphatidylserine, PI, phosphatidylinositol, CL, cardiolipin, Sph, sphingomyelin, bis-PA, *bis*-phosphatidic acid. (*b.2*) Cardiolipin content in BAL obtained from control mice and mice treated with *E.coli* (10^6 CFU/mouse). Data are mean SEM. **P*<0.05 vs. control, n=4. (*b.3-b.4*) Typical negative ESI-MS spectra of doubly-charged ($[M-H]^{2-}$) cardiolipin obtained from control mice (*b.3*) and mice challenged with *E. coli* (*b.4*). **c**) Molecular species of cardiolipin isolated from human and mouse BALs. The predominant molecular species were C16:1/C18:2/C18:2/C18:2, C18:1/C18:2/C18:2/C18:2 and C18:1/C18:2/C18:2/C20:4, characteristic of mammalian pulmonary CLs. In contrast, the major signature CLs of *E. coli* - C16:0/C16:1/C16:0/C18:1, C16:0/C17:1/C16:0/C18:1, C16:0/C18:1/C16:0/C18:1 and C18:1/C18:1/C16:0/C18:1 were not present in lung fluid from patients and mice infected with *E. coli*.

Analysis of cardiolipin in BAL.

Total lipids were extracted from BAL using the method described by Bligh and Dyer (1). Lipid extracts were separated and analyzed by 2D-HPTLC (2). Total lipids (60 nmol) were applied onto and the plates were first developed with a solvent system consisting of chloroform: methanol: 28% ammonium hydroxide (65:25:5 v/v). After the plates were dried with a forced N_2 blower to remove the solvent, they were developed in the second dimension with a solvent system consisting of chloroform:acetone:methanol:glacial acetic acid:water (50:20:10:10:5 v/v). The phospholipids were visualized by exposure to iodine vapors and identified by comparison with authentic phospholipid standards. Lipid phosphorus was determined by a micro-method (3). LC/ESI-MS was performed using a Dionex Ultimate™ 3000 HPLC coupled on-line to ESI and a linear ion trap mass spectrometer (LXQ Thermo-Fisher). The lipids were separated on a normal phase column (Luna 3 µm Silica 100A, 150x2 mm, (Phenomenex, Torrance CA)) with flow rate 0.2 mL/min using gradient solvents A and B. Solvent A was chloroform/methanol/28% ammonium hydroxide, 80:19.5:0.5 (v/v). Solvent B was chloroform/methanol/water/28% ammonium hydroxide, 60:34:5:0.5 (v/v). The column was eluted during the first 3 min isocratic at 0% solvent B, 3–20 min with a linear gradient from 0% solvent B to 100% solvent B, and then 20–23 min isocratic at 100% solvent B, 23–35 min linear gradient to 0% solvent B, 35–40 min isocratic at 0% solvent B for equilibrium column (4). The spectra of CL were acquired in negative mode and the scan data type was set to centroid.

References:

1. Bligh,E.G. and Dyer,W.J. 1959. A rapid method for total lipid extraction and purification. *Can.J.Biochem.Physiol.* 37:911-917.
2. Rouser G, Fkeischer S, and Yamamoto A. Two dimensional then layer chromatographic separation of polar lipids and determination of phospholipids by phosphorus analysis of spots. *Lipids* 5: 494-496, 1970.
3. Böttcher C, S,F.,, Van Gent C, M., , and Pries C. A rapid and sensitive sub-micro phosphorus determination. *Anal Chim Acta* 24: 203-4,1961.
4. Malavolta M., Bocci F., Boselli E., Frega N.G. Normal phase liquid chromatography-electrospray ionization tandem mass spectrometry analysis of phospholipid molecular species in blood mononuclear cells: application to cystic fibrosis. *J. Chromatogr. B*, 810, 173-186 (2004).

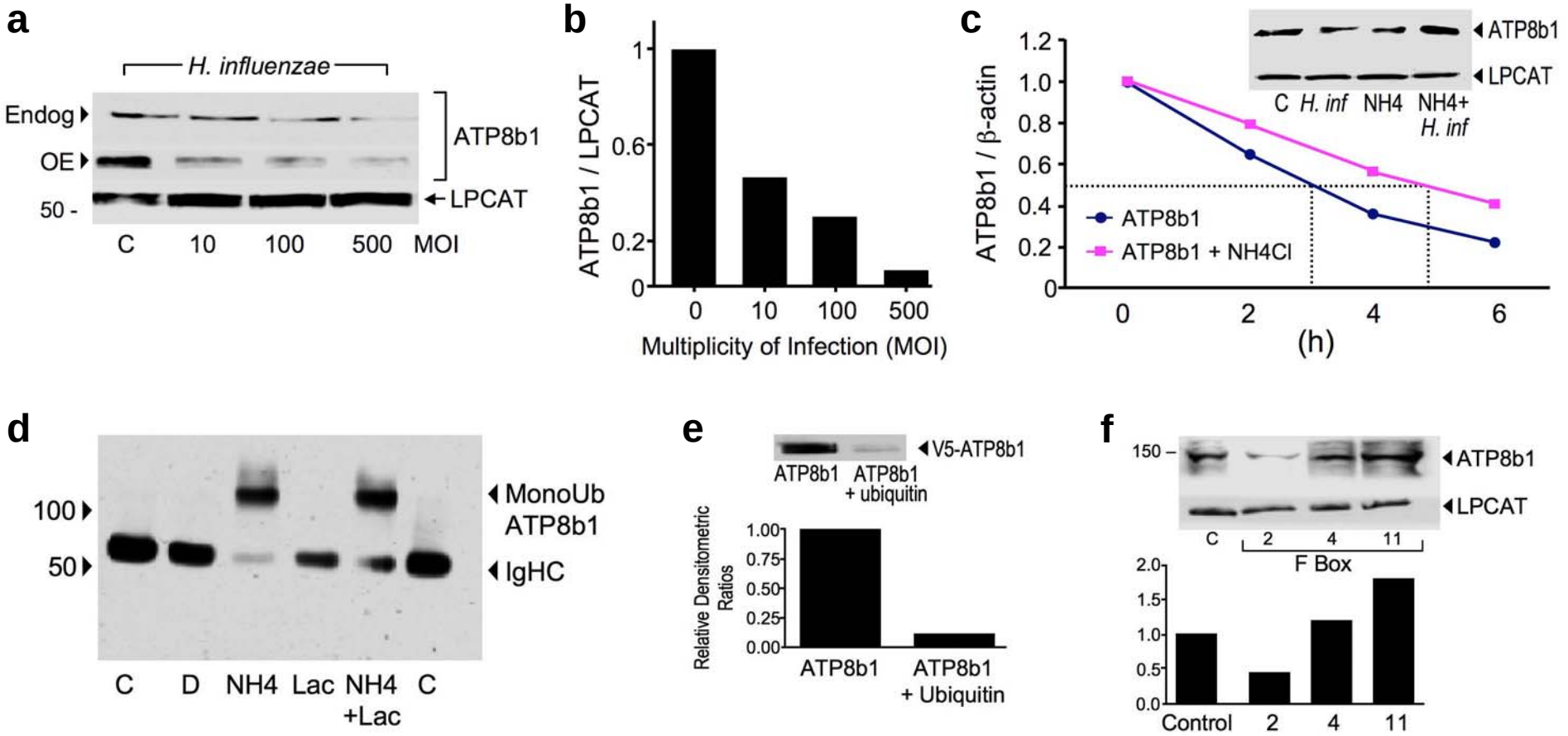

Figure 11. **ATP8b1 degradation and ubiquitination.**
a) Murine lung epithelia were exposed to various MOI of *H. influenzae* for 2 hr, harvested and processed for detection of endogenous (Endog) ATP8b1 (above) and a lipogenic (control) enzyme, LPCAT (below) by immunoblotting. The middle panel shows effects of *H. flu* on overexpressed (OE) ATP8b1 in cells. **b**) Relative amounts of ATP8b1/LPCAT were analyzed by densitometry and graphed as numeric ratios. **c**) Cells were incubated with cyclohexamide (15 mg/ml) with or without NH_4Cl (10 mM) to block lysosomal protein degradation; cells were harvested and processed for ATP8b1 immunoblotting after various times and densitometric values plotted vs. time to evaluate protein half-life. Inset: Cells were incubated with the lysosomal inhibitor, NH_4Cl (20 mM) and infected with *H. influenza* for 2 hr (MOI=100) or remained uninfected (C) prior to ATP8b1/LPCAT immunoblotting. **d**) MLE cells were transfected with V5-ATP8b1 or untransfected (C). Cells were next treated with the lactacystin carrier, DMSO (D), NH_4Cl (NH4), or proteasomal inhibitor, lactacystin (Lac). Lysates were immunopreciptitated using ubiquitin antibody and processed for SDS-PAGE and V5 immunoblot analysis to detect ATP8b1 bound to ubiquitin. The bands at ~ 55 kDa represent Ig heavy chains (IgHC). **e**) Cells were transfected with a V5-ATP8b1 with or without a construct encoding ubiquitin and cells were isolated 24 h later for V5 immunoblotting. Below: densitometric analysis of blots showing relative amounts of ATP8b1. **f**) Cells were transfected with the Skip-Cullin-FoBox (SCF) E3 ligase subunits: V5-tagged F-Box 2, 4, or 11 and harvested 24 h later for ATP8b1 (above) or LPCAT (below) by immunoblotting. Below: densitometric analysis of blots showing relative amounts of ATP8b1. The data represent n=2 separate studies.

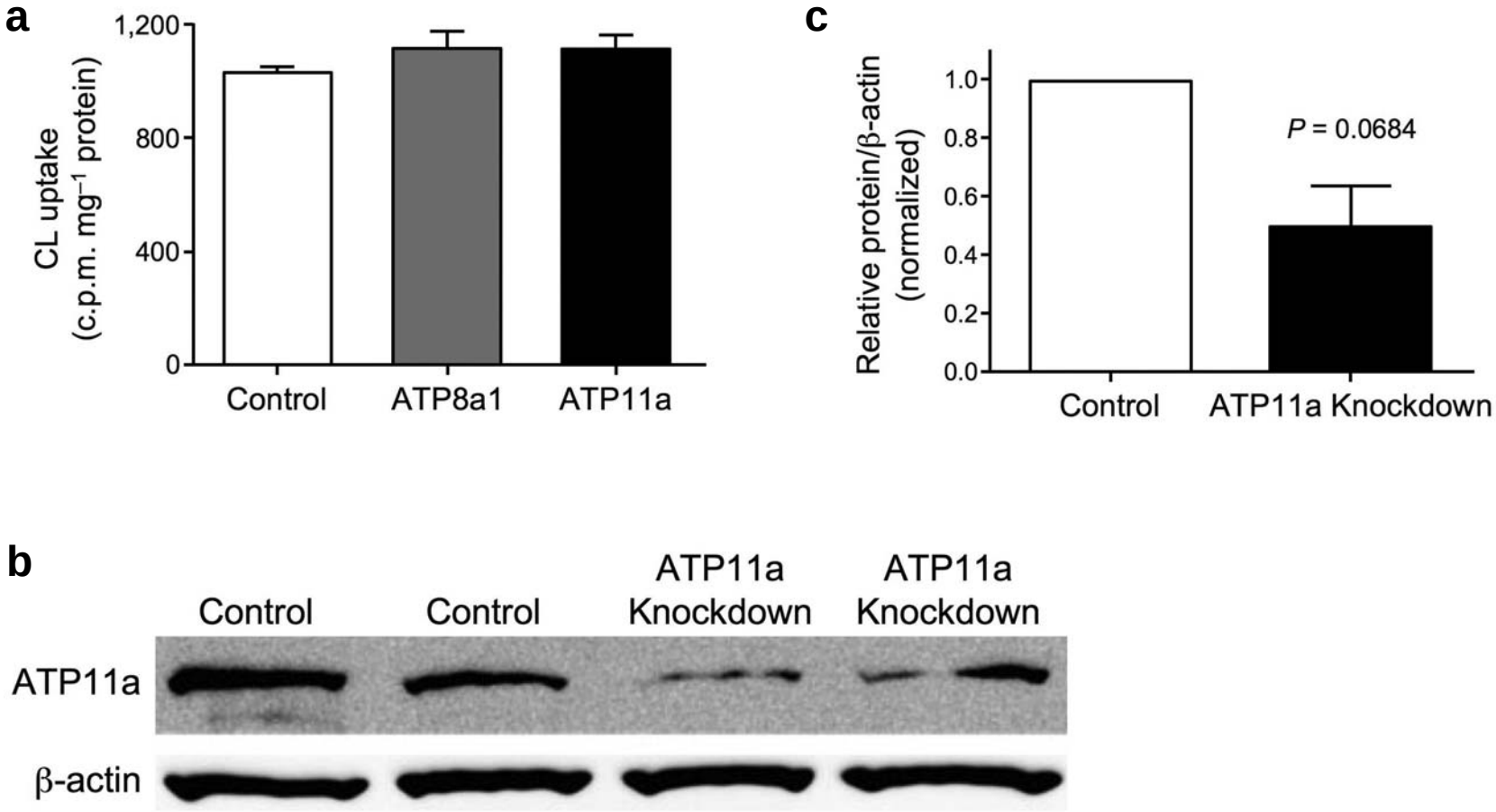

Figure 12. **Cardiolipin (CL) uptake is not regulated by related P-type ATP pumps.**
a) Cells were transfected with control, ATP8a1, or ATP11a siRNA. 24 h later cells were labeled with ^{14}C-cardiolipin for 30 min, cells harvested, and lysates and samples processed for CL uptake. The data is normalized to total cellular protein. **b**) Immunoblots showing protein levels of β-actin and ATP11a after RNAi (antibodies to ATP8a1 are not currently available). ATP8a1 mRNA levels decreased by 40% after RNAi using QPCR. **c**) Densitometry data from immunoblots (n=3) in panel **b**.

Figure 13. **Cardiolipin (CL) and CL binding domain peptide regulate cell survival pathways.**
a) Lung epithelial cells were cultured alone (control), with CL (180 nmol), with CL binding domain peptide (360 nmol), or CL in combination with CL binding domain peptide (360 nmol) for 18 h. Cells were harvested, lysates were separated using SDS-PAGE, and GSK-3β, phospho-GSK-3β, ERK1, phospho-ERK1, eIF4E (control), and β-actin (control) levels were measured by immunoblotting. **b**) Densitometric data from immunoblots in panel **a**. n=3. **P*<0.05; #*P*<0.0001 vs control. Note that administration of peptide alone or with CL markedly activates GSK-3 (dephosphorylated form) and ERK1 (phosphorylated form).

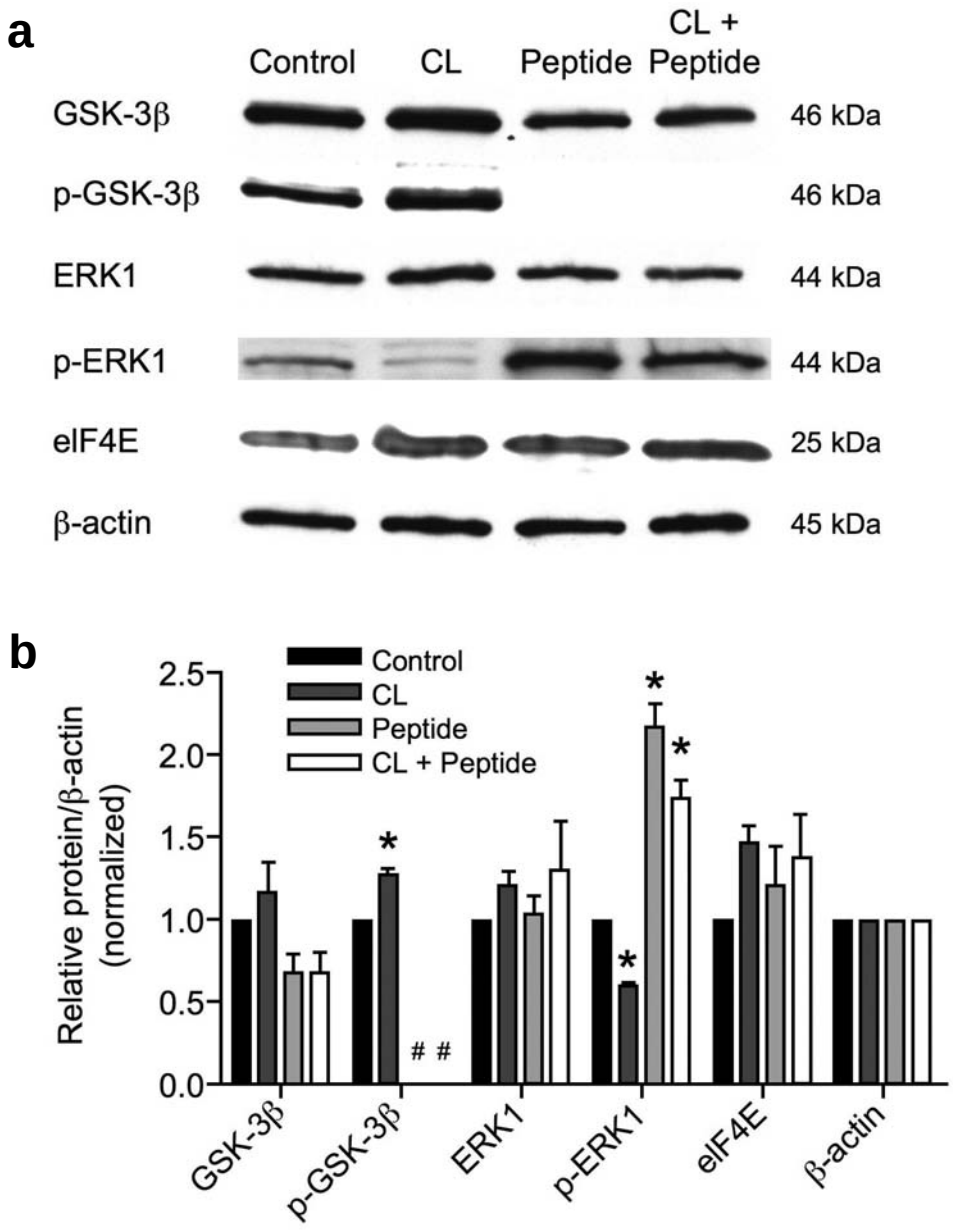

Methods

ATP8b1 expression and cloning. Real-time PCR was performed as described[33]. Total RNA was isolated from murine small intestinal mucosal cells using Tri reagent (Sigma), reverse transcribed to cDNA, and ATP8b1 amplified using an Accuscript kit (Stratagene) with ATP8b1 primers. A 4.0 kb fragment of DNA including the full-length coding sequence and the stop codon for ATP8b1 was cloned into the pENTR/D-TOPO followed by pcDNA-DEST40, pLenti6/V5-DEST, or pcDNA3.1D/V5-His (Invitrogen Gateway Cloning System). A full-length (FL) ATP8b1/ pcDNA-DEST40 clone was used to generate truncation mutants by site-directed mutagenesis using a Quik-Change II kit (Stratagene), by introduction of stop codons. NH_2-terminal deletion mutants were generated by PCR using 5' primers introducing start codons within the ATP8b1 primary sequence. PCR products were cloned into pENTR/D-TOPO followed by pcDNA-DEST40.

ATP8b1 CL binding domain (CBD) peptide. The ATP8b1 CL binding domain (CBD) peptide (amino acids 771-850) was amplified from FL ATP8b1 in pcDNA-DEST40 with engineered BamHI sites and ligated to a GST containing fragment excised from pDEST26 (Invitrogen) using BlgII. GST-CBD or GST alone were then cloned into pcDNA3.1D/V5-His (Invitrogen) and transfected into MLE cells for expression and GST pull-downs, or used for *in vitro* transcription and translation (TnT)[33].

Confocal microscopy. Frozen lung sections fixed (2% paraformaldehyde), permeabilized with 0.1% saponin, and incubated with the primary antibodies or mouse anti-occludin followed by AlexaFlour 568 goat anti-rabbit and AlexaFluor488 chicken anti-mouse secondary antibodies, respectively (Invitrogen). Preparations were imaged using a Zeiss 510 Multiphoton/Confocal microscope (Bio-Rad).

In vitro translation. A TNT T7 coupled reticulocyte lysate system kit (Promega) including T7 polymerase and rabbit reticulocyte lysate was used for *in vitro* protein expression of ^{35}S-methione-labeled ATP8b1 FL, NH_2-terminal mutants, and ATP8b1 CBD and GST peptide clones[33].

In vivo micro-CT imaging. Lipid (CL [50 nmol, 100 nmol]) was administered through a tracheotomy, mice paralyzed, and sedation maintained during mechanical ventilation using 1.5% isofluorane. A Micro-CT II (Siemens Pre-Clinical Solutions) was used for *in vivo* scanning using a custom gated imaging process with settings of 60kVp, 500microA, and an exposure time of 500ms. A total of 720 projections were acquired over 200 degrees.

Tissue fixation. Lungs were fixed using 25% polyethylene glycol 400, 10% ethyl alcohol, 10% formaldehyde i.t. via a gravity feed system at a constant pressure (20 cmH_2O). After 30 min., lungs were removed and immersed in fixative solution for 24 h., Lungs were then air-dried for 48 h at 60 °C with 20 cmH_2O air pressure applied at the trachea. *Ex vivo* imaging was acquired at 60kVp, 368 microA and an exposure of 2250 ms. A total of 720 projections were acquired over 200 degrees.

Lipid overlay. Lipid strips (Echelon Biosciences, Inc.) were incubated with translation products in TTBS buffer with 1% fatty acid-free BSA. Strips were washed extensively and radiolabeled protein was detected with V5 antibody using immunoblotting.

Surface Tension. Required amounts of phospholipids (Avanti Polar Lipids, Inc.) dissolved in ethanol were dried under nitrogen. 0.25 ml of $CaCl_2$ (5 mM) solution containing 1 μmole Infasurf was added and sonicated for 10 s to incorporate the lipid into Infasurf. Apoprotein depletion was achieved by Bligh-Dyer extraction of Infasurf, reconstitution with individual phospholipids and $CaCl_2$ (5 mM), and shown to be devoid of SP-B and SP-C by immunoblotting. Dynamic minimum surface tension (γ_{min}) was measured using a pulsating bubble surfactometer[34].